AFML-TR-71-165

INFRARED DISPERSION ANALYSIS AND OPTICAL CONSTANT SPECTRA OF α-Fe_2O_3 (HEMATITE)

CONRAD M. PHILLIPPI
STEPHEN R. LYON

TECHNICAL REPORT AFML-TR-71-165

JUNE 1971

AIR FORCE MATERIALS LABORATORY
AIR FORCE SYSTEMS COMMAND
WRIGHT-PATTERSON AIR FORCE BASE, OHIO

R

41

UNCLASSIFIED

Security Classification

DOCUMENT CONTROL DATA - R & D

(Security classification of title, body of abstract and indexing annotation must be entered when the overall report is classified)

1. ORIGINATING ACTIVITY (Corporate author)	2a. REPORT SECURITY CLASSIFICATION
Air Force Materials Laboratory Wright-Patterson AFB, Ohio 45433	Unclassified
	2b. GROUP

3. REPORT TITLE

INFRARED DISPERSION ANALYSIS AND OPTICAL CONSTANT SPECTRA OF α-Fe_2O_3 (HEMATITE)

4. DESCRIPTIVE NOTES *(Type of report and inclusive dates)*

5. AUTHOR(S) *(First name, middle initial, last name)*

Conrad M. Phillippi
Stephen R. Lyon

6. REPORT DATE	7a. TOTAL NO. OF PAGES	7b. NO. OF REFS
	32	10

8a. CONTRACT OR GRANT NO.	9a. ORIGINATOR'S REPORT NUMBER(S)
b. PROJECT NO. 7360 and 7353	AFML-TR-71-165
c. Task No. 736005 and 735302	9b. OTHER REPORT NO(S) *(Any other numbers that may be assigned this report)*
d.	

10. DISTRIBUTION STATEMENT

Approved for public release; distribution unlimited

11. SUPPLEMENTARY NOTES	12. SPONSORING MILITARY ACTIVITY
	Air Force Materials Laboratory Wright-Patterson AFB, Ohio 45433

13. ABSTRACT

Infrared reflection spectra of the ordinary and extraordinary rays of single crystal ferric oxide (α-Fe_2O_3) in the form of the mineral hematite are isolated and measured. Dispersion analyses are performed on these spectra and the best-fit resonance parameters are identified, along with estimated tolerances. Longitudinal optical mode frequencies are calculated from these data. Also calculated are: refractive index, extinction coefficient, absorption coefficient, and real and imaginary parts of the dielectric constant of both rays. These are presented as tabulations between 4000 and 200 cm^{-1}, and as plots between 700 and 200 cm^{-1}. Several oxidation film spectra from pure iron are illustrated and discussed.

DD FORM 1 NOV 68 1473

UNCLASSIFIED

Security Classification

NOTICE

When Government drawings, specifications, or other data are used for any purpose other than in connection with a definitely related Government procurement operation, the United States Government thereby incurs no responsibility nor any obligation whatsoever; and the fact that the government may have formulated, furnished, or in any way supplied the said drawings, specifications, or other data, is not to be regarded by implication or otherwise as in any manner licensing the holder or any other person or corporation, or conveying any rights or permission to manufacture, use, or sell any patented invention that may in any way be related thereto.

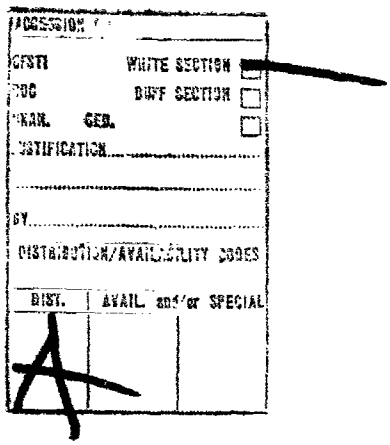

Copies of this report should not be returned unless return is required by security considerations, contractual obligations, or notice on a specific document.

AIR FORCE: 28-9-71/350

14 KEY WORDS	LINK A		LINK B		LINK C	
	ROLE	WT	ROLE	WT	ROLE	WT
Hematite						
Ferric Oxide						
Reflection Spectrum						
Dispersion Analysis						
Oxidation						

INFRARED DISPERSION ANALYSIS AND OPTICAL CONSTANT SPECTRA OF α-Fe_2O_3 (HEMATITE)

CONRAD M. PHILLIPPI
STEPHEN R. LYON

ABSTRACT

Infrared reflection spectra of the ordinary and extraordinary rays of single crystal ferric oxide (α-Fe_2O_3) in the form of the mineral hematite are isolated and measured. Dispersion analyses are performed on these spectra and the best-fit resonance parameters are identified, along with estimated tolerances. Longitudinal optical mode frequencies are calculated from these data. Also calculated are: refractive index, extinction coefficient, absorption coefficient, and real and imaginary parts of the dielectric constant of both rays. These are presented as tabulations between 4000 and 200 cm^{-1}, and as plots between 700 and 200 cm^{-1}. Several oxidation film spectra from pure iron are illustrated and discussed.

FOREWORD

This report was prepared by the Analytical Branch, Materials Physics Division, in collaboration with the Advanced Metallurgical Studies Branch, Metals and Ceramics Division, both of the Air Force Materials Laboratory, Wright-Patterson Air Force Base, Ohio. This work was conducted under Project 7360, "Chemical, Physical, and Thermodynamic Properties of Aircraft, Missile, and Spacecraft Materials", Task 736005, "Compositional, Atomic, and Molecular Analysis of Experimental Materials for Advanced Air Force Systems", and Project 7353, "Characterization of Solid Phase and Interphase Phenonema in Crystalline Substances", Task 735302, "Correlation of Physical and Mechanical Properties of Metals and Ceramics", by Conrad M. Phillippi (LPA), Research Physicist and Stephen R. Lyon (LLS), Research Metallurgist.

This report covers work performed between June 1970 and March 1971. The manuscript was submitted by the authors in June 1971.

The authors gratefully acknowledge the contributions of David W. Fischer of the Analytical Branch for the generous loan of the hematite crystals from his collection and his continuing interest in this work.

The work described herein is a selected part of a general study into the application of infrared and Raman spectroscopic techniques to the characterization of oxidation and corrosion products and processes of Air Force metals and alloys. Ferric oxide is a prominent oxidation product of ferrous alloys.

This technical report has been reviewed and is approved.

Freeman F. Bentley

FREEMAN F. BENTLEY, Chief
Analytical Branch
Materials Physics Division

TABLE OF CONTENTS

ILLUSTRATIONS

INTRODUCTION

The oxidation and corrosion products of Air Force metals and alloys are particularly amenable to study by infrared spectroscopic techniques. The realtime characterization of oxidation films growing *in situ* by means of infrared reflection spectroscopy is being developed by this laboratory (Ref 1). To characterize such a film it is necessary to know 1) its optical constant spectra and 2) the assignment of various spectroscopic features to specific vibrational species of its crystal lattice. Optical constant data are used in equations to quantitatively describe the physical properties of films (thickness, orientation, homogeneity) from spectroscopic measurements. Vibrational assignments are necessary for identifying the various oxides in multi-component films and for resolving anomalies which appear in the oxidation spectra of new alloy systems. This is especially important where the films are optically anisotropic and may exhibit preferential orientation effects.

In the characterization of oxidation films on ferrous alloys, α-Fe_2O_3 is one of the oxides frequently encountered. In the mineral form, this oxide is hematite and it occurs as large single crystals with surfaces suitable for direct measurement of optical properties. With appropriate precautions, a single crystal may be considered to be an infinitely thick oriented oxidation film. The optical constants, therefore, of the bulk single crystal can be used as a first approximation to those of an oxidation film. In this study, natural crystal faces were measured to avoid possible spectral changes due to lattice damage from the optical grinding and polishing required to prepare oriented artificial surfaces.

Several large natural single crystals of hematite from Goyaz, Brazil, were available for measurement. The black metallic-like crystals displayed large

well-developed smooth faces, several of which were perpendicular to, and nearly parallel to, the optic axis. These surfaces observed by reflection in nearly normally incident polarized radiation were sufficient for isolation of the ordinary (ω) and extraordinary (ε) ray spectra. In effect (Ref 2) these spectra are associated with lattice vibrations perpendicular to and parallel to the optic axis, respectively. The impurities in the crystal used for primary measurements, as determined by emission spectroscopy, are listed in Table I.

α-Fe_2O_3 belongs to the rhombohedral system and can be referenced to either rhombohedral or hexagonal crystal axes. It is described by the space group D_{3d}^6 with two Fe_2O_3 molecules in the rhombohedral unit cell (Ref 3). A factor group analysis for k=0 predicts the following optical activity (Ref 4):

Infrared active	2 A_{2u} (E∥C) 4 E_u (E⊥C)
Raman active	2 A_{1g} 5 E_g
Optically inactive	2 A_{1u} 3 A_{2g}

Of importance to these measurements is the expectation of finding two infrared active fundamental modes in the ε-ray (E∥C) and four more in the ω-ray (E⊥C). Ferric oxide is isomorphous with the sesquioxides of aluminum, chromium, gallium, rhodium, titanium, and vanadium, and these modes have been isolated and assigned in at least Al_2O_3 (Ref 5) and Cr_2O_3 (Ref 6).

EXPERIMENTAL

The double-beam spectrometer employed in these measurements is a PE Model 225 infrared grating spectrophotometer which covers the range 4000 to 200 cm^{-1}. The sample beam intensity is so great that absorbing samples such as these hematite crystals reach equilibrium temperatures on the order of 80°C. The spectrometer is equipped with a wire grid polarizer located at the entrance slit to the foreprism monochromator and common to both beams. Having an AgBr substrate its useful range of transmission extends only to 280 cm^{-1}, and so spectra from 280 to 200 cm^{-1} were measured in unpolarized radiation.

The specular reflectance attachment inserted in the sample beam is shown in Fig. 1. The average angle of incidence is 15°. With no similar attachment in the reference beam there is some unbalance at the atmospheric absorption lines but this is minimized by purging the instrument with dry nitrogen. Furthermore, the 100% line is not flat and this effect is compensated by measuring sample reflectances relative to those of an evaporated gold mirror in the same position. In these particular measurements no correction was made for mirror reflectances being less than unity, because this error tends to compensate for scattering losses from the less-than-perfect crystal faces. The sample is mounted on a 6-degree of freedom goniometer, enabling precise positioning of a surface in the beam. Measurement procedure consisted of 1) mounting a crystal face in the goniometer with the optic axis in a selected orientation relative to the plane of incidence 2) adjusting the orientation of the face for peak reflected signal 3) selecting the plane of polarization relative to the plane of incidence 4) scanning the sample reflection spectrum and repeating with the mirror substituted for the sample 5) reading the two spectra

at intervals of 5 cm^{-1} or less depending on steepness, and calculating the reflection coefficient as the ratio.

Fig. 2 illustrates the optical configurations by means of which the ordinary and extraordinary ray spectra may be isolated, assuming faces parallel to and perpendicular to the optic axis are available. Four of these configurations isolate a ray independently of the angle of incidence; they are ε= S:S and ω= N:S = S:P = P:S. To provide an alternate configuration for confirmation of extraordinary ray isolation, ε = P:P(0) can also be approximated by a 15° angle of incidence (P:P(15°)).

A natural face parallel to the optic axis (necessary for the P:S, S:P, S:S, and P:P(0) configurations) and large enough to fill the sample beam for absolute reflectances was not present on these crystals. However, a small face inclined at an angle of only 10° 8' to the optic axis, as determined by optical goniometric measurement, was found which enabled the above configurations to be approximated. Using this face, ω and ε-ray spectra could be isolated but absolute reflectances could not be measured accurately. However, as described below, absolute reflectances were determined from amply large (0006) and $(11\bar{2}3)$ faces.

Fig. 3 shows the full unpolarized reflection spectrum from a pyramidal face; this is a mixture of ω and ε spectra. The frequencies of the three minima and one maximum are approximate and are so designated for discussion purposes. The 500 cm^{-1} minimum was found between 500.5 and 495 cm^{-1} off various faces and polarizations, the 412 cm^{-1} minimum appeared between 411 and 413 cm^{-1}, and the 370 cm^{-1} minimum appeared between 372 and 368.5 cm^{-1}. The 230 cm^{-1} maximum was comparatively invariant. Fig. 4 shows the polarized reflection spectrum from a (0006) face perpendicular to the optic axis (solid curve). This spectrum is the same in N:S and N:P configurations at 15° angle of incidence. On this basis the 500 and 370 cm^{-1} minima are assigned to the ordinary ray. The broken curve in

Fig. 4 shows the S:S polarized spectrum off the small face inclined 10° 8' to the optic axis. In this the 500 cm^{-1} minimum is completely missing and the single minimum at 412 cm^{-1} appears. This same spectrum is also obtained in the P:P (15°) configuration and on this basis the 412 cm^{-1} minimum is assigned to the extraordinary ray. Additionally, the ordinary ray spectrum was confirmed in the P:S and S:P configurations from this latter face.

At this point, two extraordinary and three ordinary bands are now assigned. However, a fourth ordinary band is expected. The spectral region between 200 and 50 cm^{-1} was searched using a PE #301 far infrared grating spectrophotometer for additional modes. Powdered ferric oxide blended in polyethylene pellets at both the 10 and 30 weight percent concentrations was examined in transmission but no bands were found. The powder transmission technique was used for this search because it assures reflection bands will not be missed inadvertently by polarization effects and because it allows very weak bands to be sought by control of concentrations. Therefore, the weak band at 230 cm^{-1} is assumed to be the remaining fundamental and it is assigned to the ordinary ray on the basis of expectation.

The absolute reflectance spectrum of the ordinary ray is obtained directly from measurements on the (0006) face. The extraordinary ray from a second-order pyramidal face $(11\bar{2}3)$ is most nearly isolated when both the optic axis and the electric vector of incident radiation lie in the plane of incidence and the optic axis lies on the reflected beam side. Under these conditions the electric vector is inclined to the optic axis by only about 27°. The spectrum of this face with the ordinary ray components pencilled out, is taken to be the absolute reflectance spectrum of the extraordinary ray.

DISPERSION ANALYSIS

The multiresonance damped classical oscillator model is used to curve fit the ordinary and extraordinary spectra independently. This theory assumes the

measured reflection spectrum can be approximated by the dielectric properties of a medium containing j kinds of classical oscillators each described by a resonant frequency, a strength factor, and a damping factor. Following are the definitions of terms and mathematical essentials of this theory:

$$\hat{\epsilon} = \epsilon_\infty + \sum_j \frac{\rho_j \nu_j^2}{\nu_j^2 - \omega^2 + i\gamma_j \omega} \tag{1}$$

$$\hat{\epsilon} = \hat{n}^2 = n^2 - 2ink - k^2 \tag{2}$$

$$n^2 - k^2 = \epsilon_\infty + \sum_j \frac{\rho_j \nu_j^2 (\nu_j^2 - \omega^2)}{(\nu_j^2 - \omega^2)^2 + \gamma_j^2 \omega^2} \tag{3}$$

$$2nk = \sum_j \frac{\omega \rho_j \gamma_j \nu_j^2}{(\nu_j^2 - \omega^2)^2 + \gamma_j^2 \omega^2} \tag{4}$$

$$R = \frac{(n-1)^2 + k^2}{(n+1)^2 + k^2} \tag{5}$$

where

$\hat{\epsilon}$ = complex dielectric constant

ϵ_∞ = real dielectric constant at infinitely high frequency

ρ_j = strength of the j-th oscillator

ν_j = resonant frequency of the j-th oscillator

ω = radiation frequency

γ_j = damping factor of the j-th oscillator

$\hat{n}$ = complex refractive index

n = real refractive index

k = extinction coefficient

R = normal incidence reflection coefficient

Equation (5) is modified for non-normal incidence and the attendant polarization effects (Ref 7).

Dispersion analysis is performed by time-shared computation according to the method described in Ref 8. It is performed in real time at an ASR-35 teletype terminal to a remote digital computer. The essential features of this method are: a measured spectrum of 30 or 40 points is entered at the terminal via punched paper tape, a trial solution consisting of assumed sets of oscillator parameters is entered, and the computer then displays a calculated reflectance spectrum superposed over the measured spectrum as a low resolution line printer plot. The quality of fit is judged and a new trial solution is entered, and this process is iterated until further improvements in fit cannot be realized.

High frequency dielectric constants of 8.65 and 10.37 were used for the ϵ and ω rays, respectively. These are the squares of the refractive indices at the Na D lines for the mineral hematite according to Ref. 9.

The best-fit calculated spectra and the absolute reflectance spectra used for the dispersion analysis are presented in Fig. 5. The resonance parameters associated with these solutions, and estimated accuracies, are presented in Table I. In addition to the 2 fundamentals expected in the ϵ-ray spectrum, a "forbidden" mode is found at 545 cm^{-1} for which rough values of oscillator parameters have been tabulated. Similarly a forbidden mode at 590 cm^{-1} is observed in the ω-ray spectrum but its oscillator parameters could not be approximated. Departure from good fit around the 550 and 450 cm^{-1} reflection maxima of the ϵ and ω spectra, the 700 cm^{-1} reflection minima, and at the shorter wavelengths, are attributed to scattering imperfections of the surface and/or inadequacy of the theory underlying the dispersion equations used.

Accuracies of the best-fit resonance parameters are estimated by studying the degradation of fit as the parameters are changed one at a time. This, of course, is only an approximate method because all of the parameters interact

and influence the fit at any frequency. From Table II it is seen that most of the oscillator frequencies may be located quite accurately even though the bands are broad, while the strength and damping factors can be determined with less certainty.

OPTICAL CONSTANT SPECTRA

The various optical and dielectric constant spectra of the ε and ω rays are obtained by reinserting the best-fit resonance parameters into equations (3) and (4) and solving for the refractive index and extinction coefficient at each frequency. From these, the other constants are derived according to the following equations:

Absorption coefficient	$\alpha = 4\pi\nu k$	(6)
Conductivity	$\sigma = \nu n k$	(7)
Complex dielectric constant	$\hat{\varepsilon} = \mathrm{Re}(\varepsilon) + i\,\mathrm{Im}(\varepsilon)$	(8)

These values are presented in Tables III, IV, and V and are also plotted in Figs. 6 and 15.

Longitudinal optical phonon frequencies associated with the TO phonons in a multi-resonance spectrum are found by solving for minima in spectrum of the modulus of the complex dielectric constant for each ray, namely

$$|\hat{\varepsilon}| = \sqrt{\mathrm{Re}(\varepsilon)^2 + \mathrm{Im}(\varepsilon)^2}$$

according to Ref 10. These are presented in Table VI. As a point of interest, the LO mode frequencies as would be obtained in a single resonance spectrum by locating the points where $\mathrm{Re}(\varepsilon) = 0$ with positive slope, both with and without damping, are included in this Table.

APPLICATION EXAMPLE

Fig. 16 illustrates how data from single crystals may be used as the starting point in the characterization of oxidation film spectra. Shown are the

reflection spectra of thin and thick films of α-Fe_2O_3 on pure iron. The thin film was prepared by oxidizing iron in air at 1400°F for 1 hour. The thick film was in fact a flake which separated from the substrate after heating in air at 1250°F for 62 hours. From the interference fringe patterns in the transparent region, film thicknesses may be calculated using the refractive index data. The 700 cm^{-1} restrahlen minimum is fairly well developed in the thick film spectrum but there is no sign of it in the thin film spectrum. The 500 cm^{-1} ω-ray minimum is present in both but it is 15 cm^{-1} closer to the TO mode frequency in the thin film spectrum. The thin film spectrum shows only the ε-ray 412 cm^{-1} minimum, but more complicated structure is found in the thick film spectrum. In addition to the minimum at 392 cm^{-1}, characteristic of neither ray, weak minima at 416 and 372 cm^{-1} characteristic of both rays are found. This suggests perferential orientation effects in the thick film which may be elucidated with polarization measurements. The 235 cm^{-1} band is more prominent in the thin film spectrum. With both absorption and reflection processes operating in these spectra a full characterization will require further study. Current work in this laboratory on the oxidation spectra of a variety of alloys indicates that film thickness, grain orientation, measurements and compound identification, and multi-layer film analysis may be performed by this technique.

REFERENCES

1. Lyon and Phillippi, to be published.
2. Principles of Optics, Born and Wolf, Third Revised Edition, 1965, Pergamon Press.
3. Crystal Structures of Minerals, Bragg, Claringbull, and Taylor, 1965, Cornell University Press.
4. "Raman Effect in Relation to Crystal Structure," Bhagavantam and Venkatarayudu Proc. Indian Acad. Sciences, Vol. 9A, 1939, p244.
5. "Infrared Lattice Vibrations and Dielectric Dispersion in Corundum," A.S. Barker, Jr., Phys. Rev. Vol. 132, Nr 4 15 Nov 1964, p 1414.
6. "Infrared Lattice Vibrations and Dielectric Dispersion in Single-Crystal Cr_2O_3." Renneke and Lynch, Physical Review, Vol. 138, Nr. 2A, 19 Apr 1965, pA530.
7. Fundamentals of Optics, Jenkins and White, Third Edition, 1957, McGraw-Hill, NY.
8. "Infrared Dispersion Analysis by Time-Shared Computation", Phillippi, AFML-TR-69-256, October 1969.
9. Dana's System of Mineralogy, Palache, Berman, and Frondel, Vol. I, John Wiley & Sons, 7th Edition, 1966.
10. Long-Wavelength Longitudinal Phonons of Multi-Mode Crystals, Chang, Mitra, Plendl, and Mansur, Phys. Stat. Sol., Vol. 28, p 633, 1968.

TABLE I

EMISSION SPECTROGRAPHIC ANALYSIS OF HEMATITE

AFML/LPA Analysis

Element	Weight Percent
Ti	0.7 to 1.3
Mn	0.06 to 0.1
V	0.01 to 0.03
Al	0.007 to 0.01
Cr	0.001 to 0.003
Co	ND/less than 0.003
Si	ND/less than 0.003
Ni	ND/less than 0.001

TABLE II

RESONANCE PARAMETERS OF α-Fe_2O_3

RAY	FREQUENCY	STRENGTH	DAMPING
Extraordinary	510 $\pm$1cm^{-1}	3 $\pm$ 0.3	9 $\pm$ 3 cm^{-1}
ε_∞ = 8.65	300 $\pm$ 1	15 $\pm$ 0.5	15 $\pm$ 3
forbidden	545 $\pm$ 5	0.5*	60*
Ordinary	520 $\pm$ 2	1.5 $\pm$ 0.2	21 $\pm$ 3
ε_∞ = 10.37	435 $\pm$ 10	4.2 $\pm$ 0.3	10 $\pm$ 4
	297 $\pm$ 5	17 $\pm$ 0.5	12 $\pm$ 2
	235 $\pm$ 2	0.6 $\pm$ 0.05	3 $\pm$ 0.5
forbidden	590	small	large

* Estimated accurate to within a factor of 2

TABLE III

OPTICAL CONSTANT SPECTRA OF α-Fe_2O_3 IN THE TRANSPARENT REGION

ORDINARY RAY

```
INPUT HFDC, NR PTS, NR ØSC
8.65,20,2,
INPUT RHØ, NU, GAMMA
15.,300.,15.,
3.,510.,9.,
```

FREQ	REFR IND	EXT CØEF	ABS CØEF	CØND'TY	RE(D.C.)	IM(D.C.)
4000.0	2.918	.000	3.72	.86	8.52	.00
3750.0	2.915	.000	4.25	.99	8.50	.00
3500.0	2.911	.000	4.91	1.14	8.47	.00
3250.0	2.906	.000	5.72	1.32	8.45	.00
3000.0	2.900	.000	6.76	1.56	8.41	.00
2750.0	2.892	.000	8.12	1.87	8.36	.00
2500.0	2.881	.000	9.94	2.28	8.30	.00
2250.0	2.866	.000	12.47	2.84	8.22	.00
2000.0	2.845	.001	16.13	3.65	8.10	.00
1800.0	2.821	.001	20.43	4.59	7.96	.01
1600.0	2.786	.001	26.82	5.95	7.76	.01
1400.0	2.733	.002	37.04	8.06	7.47	.01
1200.0	2.644	.004	55.28	11.63	6.99	.02
1000.0	2.472	.008	94.73	18.64	6.11	.04
950.0	2.403	.009	112.51	21.52	5.77	.05
900.0	2.315	.012	136.92	25.22	5.36	.06
850.0	2.198	.016	172.34	30.14	4.83	.07
800.0	2.036	.023	228.26	36.98	4.14	.09
750.0	1.793	.035	329.90	47.08	3.22	.13
700.0	1.375	.066	580.55	63.52	1.89	.18

EXTRAORDINARY RAY

```
INPUT HFDC, NR PTS, NR ØSC
10.37,20,4,
INPUT RHØ, NU, GAMMA
17.,297.,12.,
4.2,435.,10.,
1.5,520.,21.,
.6,235.,3.,
```

FREQ	REFR IND	EXT CØEF	ABS CØEF	CØND'TY	RE(D.C.)	IM(D.C.)
4000.0	3.193	.000	4.33	1.10	10.20	.00
3750.0	3.190	.000	4.94	1.25	10.17	.00
3500.0	3.185	.000	5.71	1.45	10.14	.00
3250.0	3.179	.000	6.66	1.68	10.11	.00
3000.0	3.172	.000	7.88	1.99	10.06	.00
2750.0	3.163	.000	9.47	2.38	10.00	.00
2500.0	3.150	.000	11.61	2.91	9.92	.00
2250.0	3.133	.001	14.59	3.64	9.81	.00
2000.0	3.108	.001	18.94	4.68	9.66	.00
1800.0	3.080	.001	24.06	5.90	9.49	.01
1600.0	3.039	.002	31.75	7.68	9.24	.01
1400.0	2.977	.003	44.18	10.47	8.86	.01
1200.0	2.873	.004	66.77	15.26	8.25	.03
1000.0	2.675	.009	117.04	24.91	7.16	.05
950.0	2.595	.012	140.25	28.96	6.73	.06
900.0	2.494	.015	172.54	34.24	6.22	.08
850.0	2.360	.021	220.18	41.36	5.57	.10
800.0	2.177	.030	296.82	51.42	4.74	.13
750.0	1.906	.047	439.25	66.63	3.63	.18
700.0	1.446	.091	799.50	92.02	2.08	.26

TABLE IV

OPTICAL CONSTANT SPECTRA OF α-Fe_2O_3 W-RAY IN THE RESTRAHLEN REGION

INPUT HFDC, NR PTS, NR OSC
10.37,54,4,
INPUT RHO, NU, GAMMA
17.,297.,12.,
4.2,435.,10.,
1.5,520.,21.,
.6,235.,3.,

FREQ	REFR IND	EXT COEF	ABS COEF	CONDTY	RE(D.C.)	IM(D.C.)
700.0	1.446	.091	799.50	92.02	2.08	.26
690.0	1.307	.110	954.21	99.25	1.70	.29
680.0	1.138	.139	1188.31	107.57	1.27	.32
670.0	.922	.190	1598.24	117.24	.81	.35
660.0	.634	.307	2550.25	128.61	.31	.39
650.0	.355	.616	5030.24	142.14	-.25	.44
640.0	.255	.971	7805.55	158.50	-.88	.50
630.0	.222	1.275	10095.96	178.64	-1.58	.57
620.0	.212	1.554	12107.72	203.98	-2.37	.66
610.0	.213	1.824	13978.55	236.68	-3.28	.78
600.0	.223	2.095	15795.71	280.27	-4.34	.93
590.0	.243	2.378	17629.30	340.73	-5.59	1.16
580.0	.276	2.682	19551.33	428.99	-7.12	1.48
570.0	.329	3.023	21653.11	566.78	-9.03	1.99
560.0	.419	3.420	24069.89	802.39	-11.52	2.87
550.0	.586	3.910	27021.41	1259.87	-14.94	4.58
540.0	.946	4.544	30835.31	2322.29	-19.75	8.60
530.0	1.894	5.289	35223.55	5310.25	-24.38	20.04
520.0	3.942	4.826	31538.15	9893.04	-7.76	38.05
510.0	4.001	2.598	16648.85	5301.06	9.26	20.79
500.0	2.633	1.805	11340.46	2375.86	3.67	9.50
490.0	1.339	2.222	13680.16	1457.68	-3.14	5.95
480.0	.781	3.235	19513.46	1212.17	-9.86	5.05
470.0	.667	4.269	25214.11	1338.40	-17.78	5.70
460.0	.791	5.473	31639.03	1990.44	-29.33	8.65
450.0	1.354	7.254	41018.82	4418.70	-50.78	19.64
440.0	4.420	10.426	57648.04	20276.56	-89.17	92.17
435.0	9.599	9.586	52399.10	40024.94	.25	184.02
430.0	10.548	4.418	23871.44	20037.96	91.75	93.20
420.0	7.426	1.326	7000.64	4137.18	53.39	19.70
410.0	5.669	.752	3873.04	1747.14	31.57	8.52
400.0	4.468	.596	2995.78	1065.10	19.61	5.33
390.0	3.412	.612	2998.06	814.06	11.27	4.17
380.0	2.243	.858	4099.20	731.81	4.30	3.85
370.0	1.067	1.891	8792.98	746.58	-2.44	4.04
360.0	.733	3.209	14517.37	846.55	-9.76	4.70
350.0	.692	4.367	19207.47	1057.64	-18.59	6.04
340.0	.773	5.563	23768.95	1462.84	-30.35	8.60
330.0	.996	6.983	28959.25	2294.36	-47.78	13.91
320.0	1.519	8.919	35865.17	4334.44	-77.24	27.09
310.0	3.065	12.019	46822.78	11421.28	-135.07	73.69
300.0	10.452	15.990	60281.64	50136.77	-146.45	334.25
297.0	14.849	14.179	52918.81	62531.03	19.45	421.08
290.0	16.200	5.565	20279.44	26142.90	231.47	180.30
280.0	12.592	1.873	6589.83	6603.04	155.04	47.16
270.0	10.585	.952	3228.72	2719.58	111.13	20.15
260.0	9.366	.594	1941.39	1446.92	87.36	11.13
250.0	8.474	.434	1362.84	919.05	71.63	7.35
240.0	7.378	.583	1757.29	1031.73	54.09	8.60
235.0	8.504	2.999	8856.61	5993.19	63.32	51.01
230.0	8.576	.427	1234.52	842.54	73.37	7.33
220.0	7.758	.198	548.48	338.63	60.15	3.08
210.0	7.383	.150	396.41	232.91	54.49	2.22
200.0	7.118	.122	306.07	173.38	50.66	1.73

TABLE V

OPTICAL CONSTANT SPECTRA OF α-Fe_2O_3 c-RAY IN THE RESTRAHLEN REGION

INPUT HFDC, NR PTS, NR OSC
8.65,54,2,
INPUT RHO, NU, GAMMA
15.,300.,15.,
3.,510.,9.,

FREQ	REFR IND	EXT COEF	ABS COEF	CONDTY	RE(D.C.)	IM(D.C.)
700.0	1.375	.066	580.55	63.52	1.89	.18
690.0	1.246	.079	686.91	68.12	1.55	.20
680.0	1.088	.099	847.42	73.37	1.17	.22
670.0	.884	.134	1129.70	79.43	.76	.24
660.0	.595	.220	1826.00	86.50	.31	.26
650.0	.275	.530	4329.88	94.84	-.21	.29
640.0	.181	.903	7259.68	104.82	-.78	.33
630.0	.154	1.209	9573.79	116.97	-1.44	.37
620.0	.143	1.489	11599.22	132.05	-2.20	.43
610.0	.141	1.761	13497.79	151.20	-3.08	.50
600.0	.144	2.038	15365.89	176.24	-4.13	.59
590.0	.153	2.331	17280.93	210.11	-5.41	.71
580.0	.168	2.651	19323.92	257.99	-7.00	.89
570.0	.192	3.015	21599.22	329.54	-9.06	1.16
560.0	.230	3.448	24264.37	444.75	-11.84	1.59
550.0	.296	3.992	27591.63	650.62	-15.85	2.37
540.0	.423	4.734	32123.52	1080.44	-22.23	4.00
530.0	.720	5.879	39158.36	2243.81	-34.05	8.47
520.0	1.792	8.051	52611.60	7502.14	-61.61	28.85
510.0	9.249	9.209	59022.17	43440.83	.73	170.36
500.0	8.235	1.768	11107.03	7278.75	64.69	29.11
490.0	6.114	.707	4352.29	2117.61	36.88	8.64
480.0	4.997	.424	2555.61	1016.19	24.79	4.23
470.0	4.259	.314	1856.10	629.12	18.04	2.68
460.0	3.692	.270	1559.05	458.01	13.56	1.99
450.0	3.200	.260	1471.30	374.68	10.17	1.67
440.0	2.728	.279	1543.49	335.07	7.36	1.52
435.0	2.484	.301	1647.36	325.63	6.08	1.50
430.0	2.225	.336	1815.15	321.42	4.84	1.49
420.0	1.625	.478	2523.17	326.23	2.41	1.55
410.0	.903	.937	4825.81	346.94	-.06	1.69
400.0	.553	1.737	8729.19	384.20	-2.71	1.92
390.0	.466	2.429	11902.10	441.57	-5.68	2.26
380.0	.453	3.060	14612.09	526.52	-9.16	2.77
370.0	.478	3.693	17169.84	653.11	-13.41	3.53
360.0	.539	4.374	19788.18	848.21	-18.84	4.71
350.0	.647	5.156	22676.58	1167.10	-26.16	6.67
340.0	.836	6.113	26119.50	1737.22	-36.67	10.22
330.0	1.193	7.380	30602.43	2905.31	-53.03	17.61
320.0	1.992	9.223	37086.03	5878.71	-81.09	36.74
310.0	4.417	12.086	47083.57	16551.23	-126.57	106.78
300.0	12.522	11.982	45170.54	45010.92	13.24	300.07
297.0	14.221	9.174	34241.23	38749.47	118.06	260.94
290.0	13.346	4.097	14931.03	15856.78	161.32	109.36
280.0	10.898	1.712	6023.60	5223.84	115.83	37.31
270.0	9.405	.944	3203.19	2397.47	87.57	17.76
260.0	8.460	.605	1976.23	1330.37	71.20	10.23
250.0	7.808	.424	1331.11	827.12	60.79	6.62
240.0	7.332	.315	948.99	553.71	53.66	4.61
235.0	7.139	.276	813.79	462.29	50.88	3.93
230.0	6.968	.243	703.59	390.13	48.49	3.39
220.0	6.680	.194	536.51	285.20	44.58	2.59
210.0	6.447	.158	417.65	214.26	41.54	2.04
200.0	6.254	.131	330.16	164.32	39.10	1.84

TABLE VI

LONGITUDINAL OPTICAL PHONON FREQUENCIES OF α-Fe_2O_3

RAY	TO MODE	LO MODE[1]	LO MODE[2]	LO MODE[3]
ϵ	510 cm^{-1}	655 cm^{-1}	654 cm^{-1}	654 cm^{-1}
	300	410.6	410.5	410.2
ω	520	655	654.5	654.5
	435	491.5	492.5	494.7
	297	373.7	373.5	373.6
	235	237.2	236.1	236.4[4]

Notes:

1) Frequencies of minima in the spectra of the modulus of the complex dielectric constant

2) Frequencies of zeroes in the spectra of the real part of the dielectric constant, assuming zero damping for each resonance

3) Frequencies of zeroes in the spectra of the real part of the dielectric constant, using the damping factors for each resonance found in the best fit solution

4) No zero; this is the frequency of the minimum

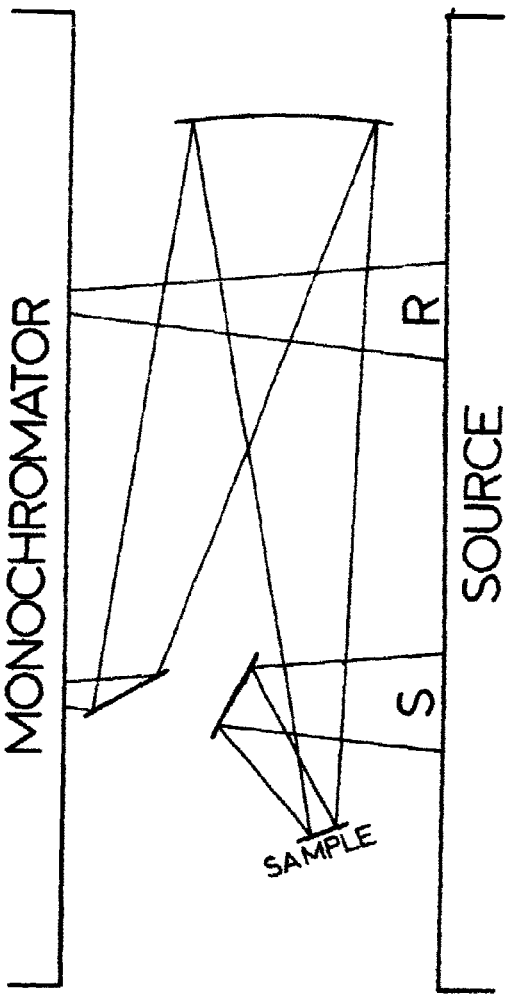

Fig. 1. Specular Reflectance Attachment for PE #225 Sample Compartment

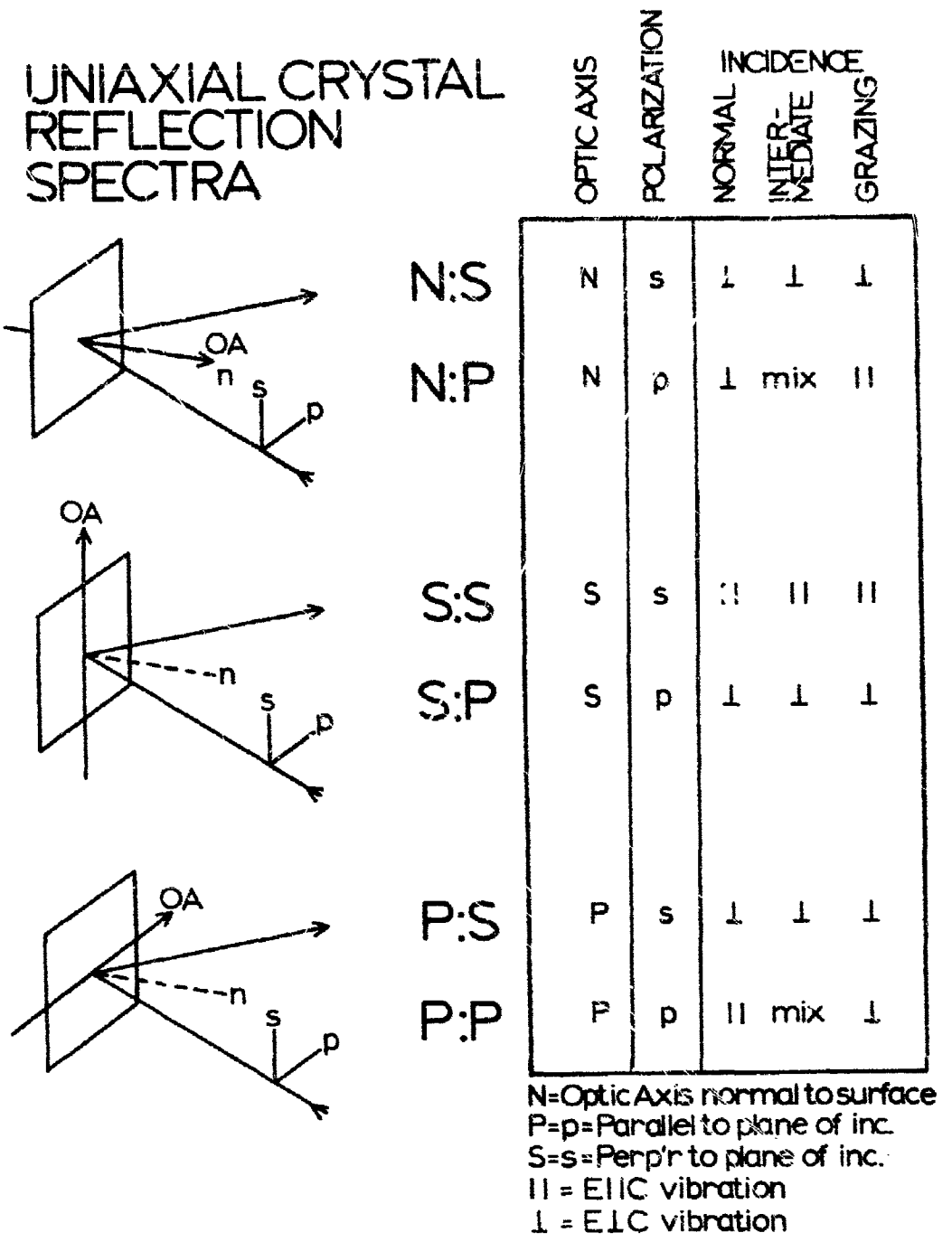

Fig. 2. Optical Geometry for Isolating Ordinary and Extraordinary Ray Spectra of Uniaxial Crystals

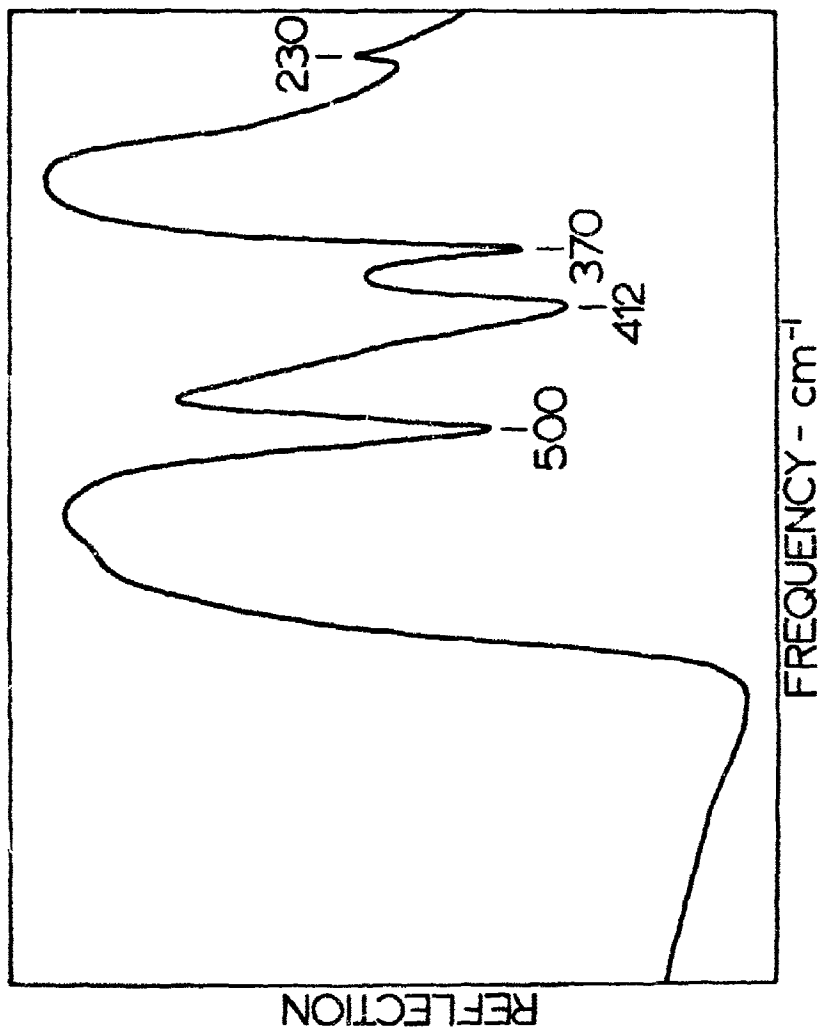

Fig. 3. Unpolarized Reflection Spectrum From Pyramidal Face of Hematite

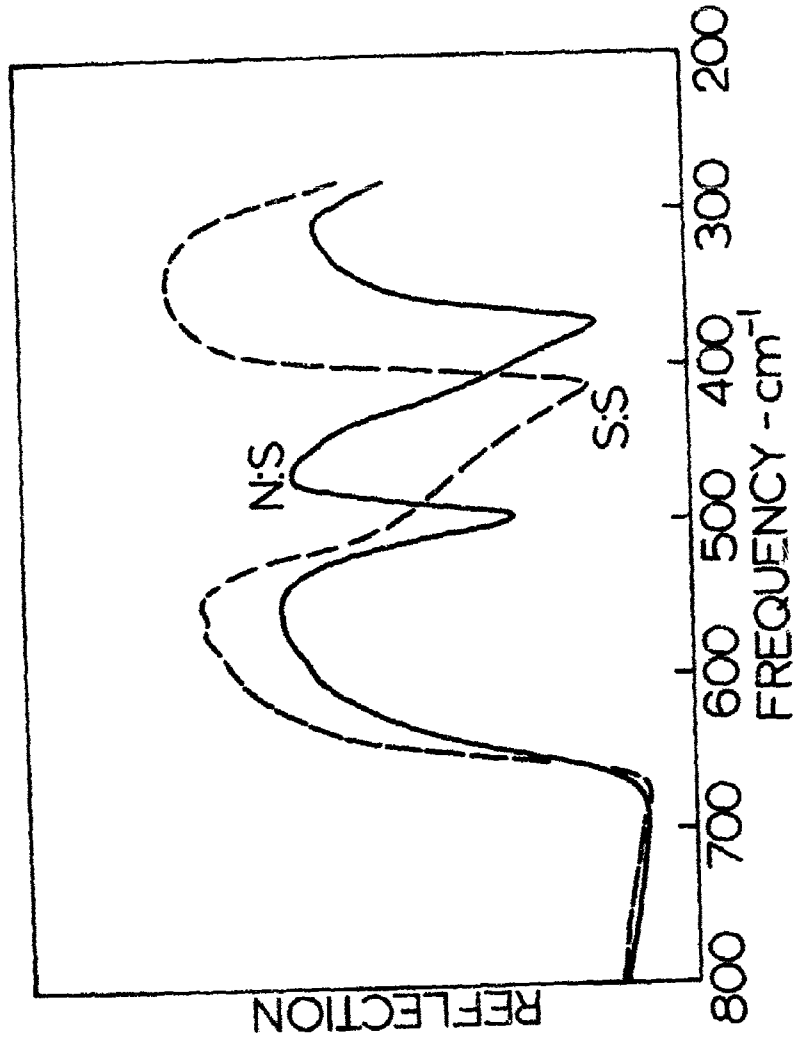

Fig. 4. Ordinary and Extraordinary Reflection Spectra of Hematite

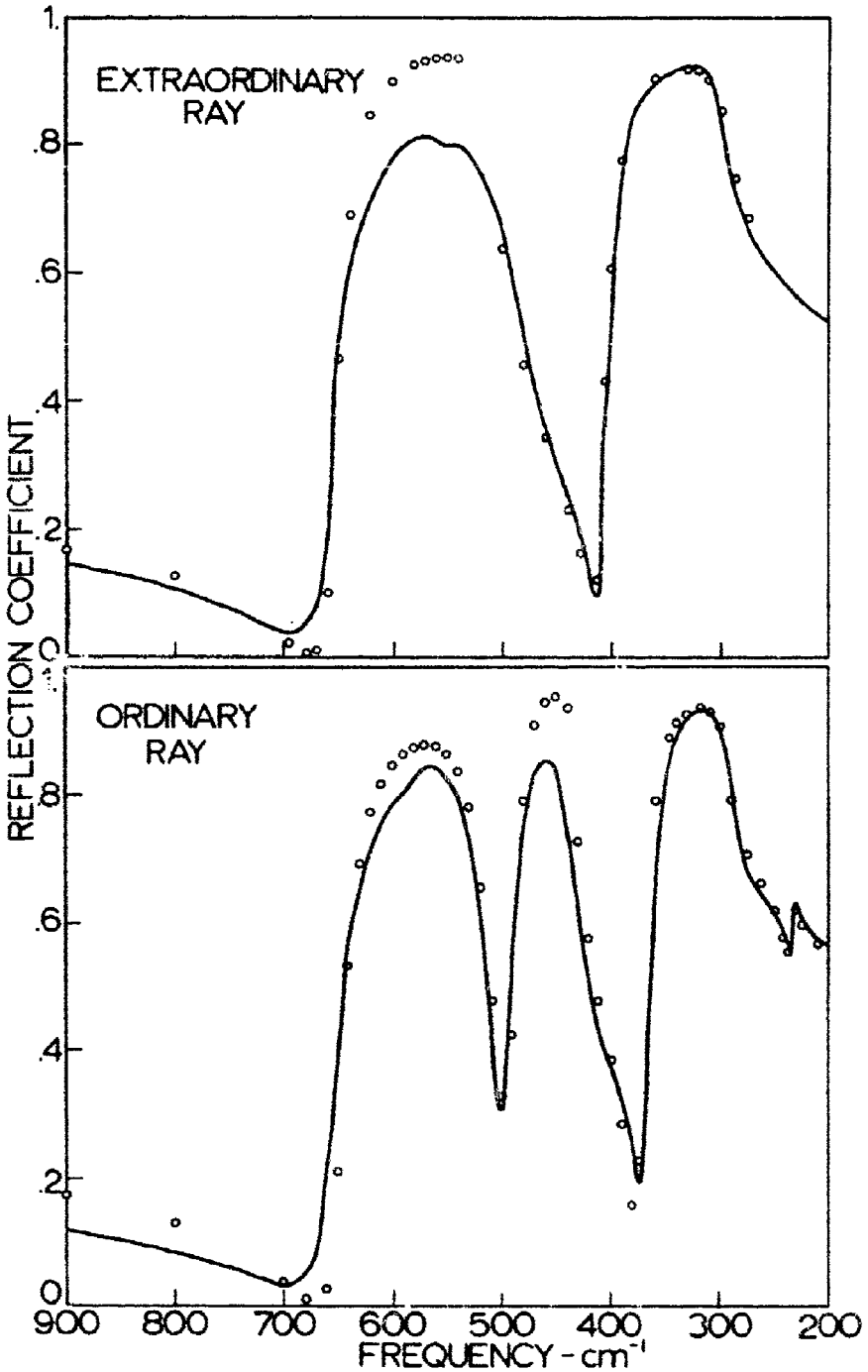

Fig. 5. Measured (Solid Line) and Best Fit Calculated (Circles) Ordinary and Extraordinary Reflection Spectra of Hematite

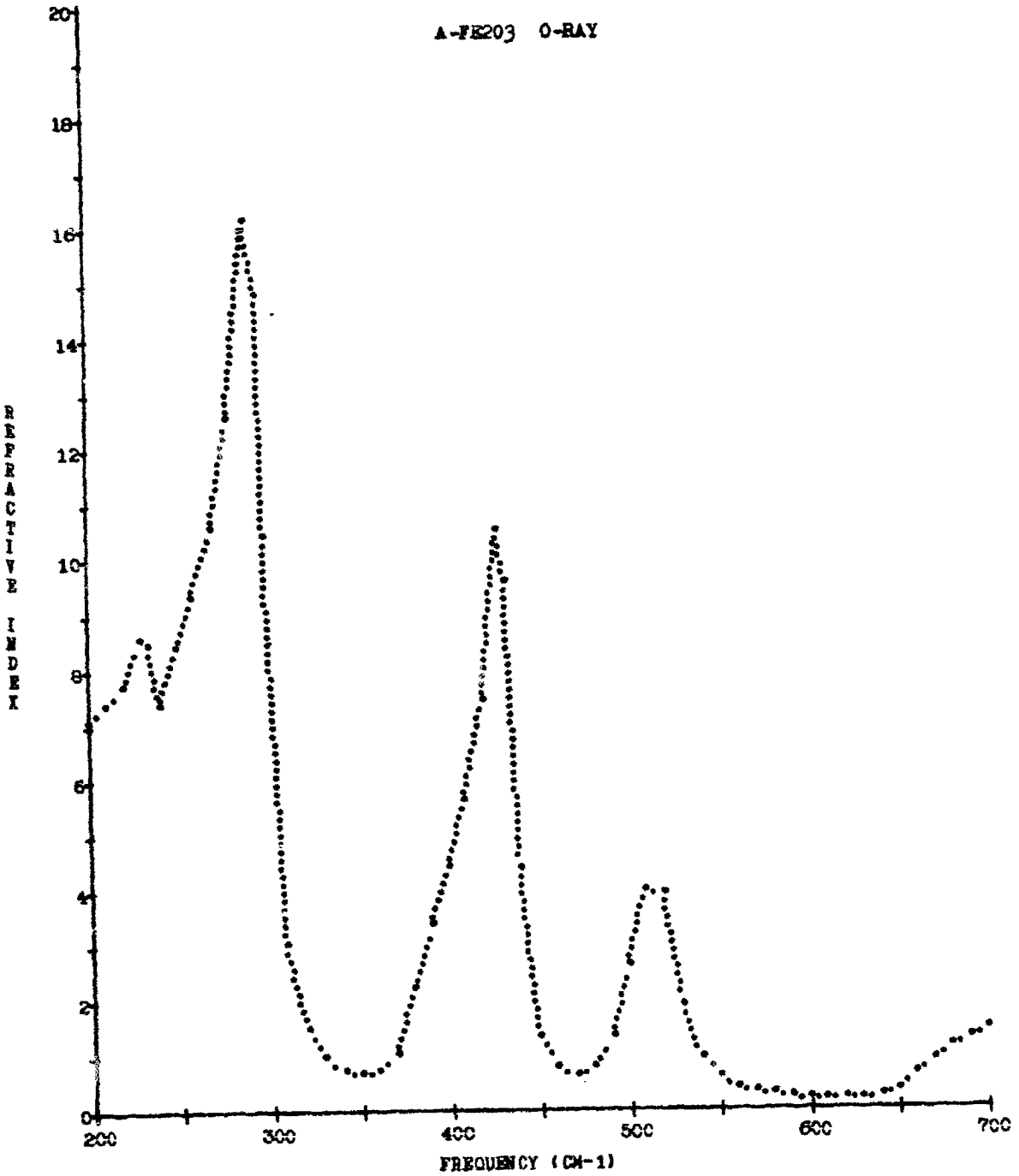

Fig. 6. Refractive Index Spectrum of Ordinary Ray of Hematite

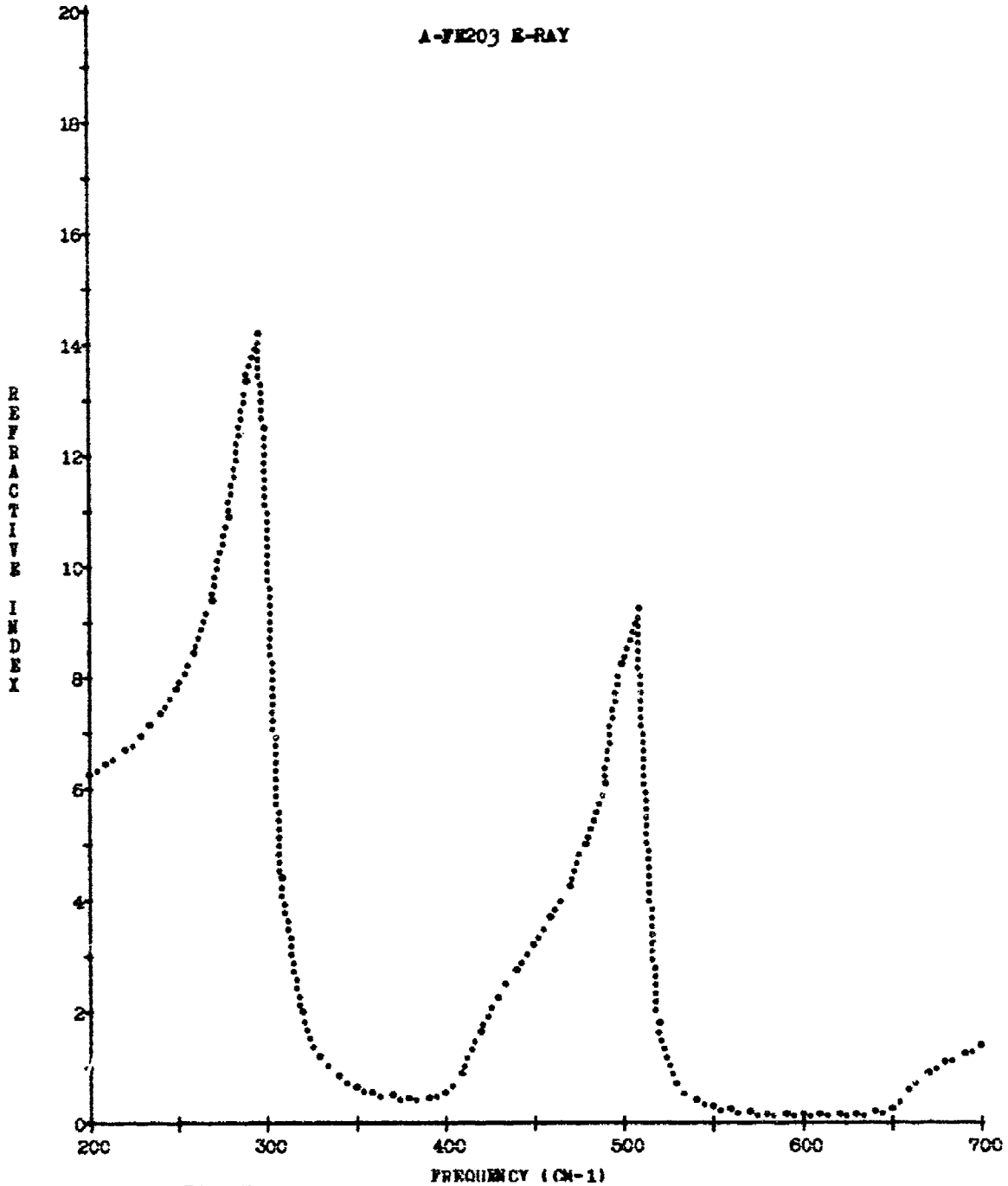

Fig. 7. Refractive Index Spectrum of Extraordinary Ray of Hematite

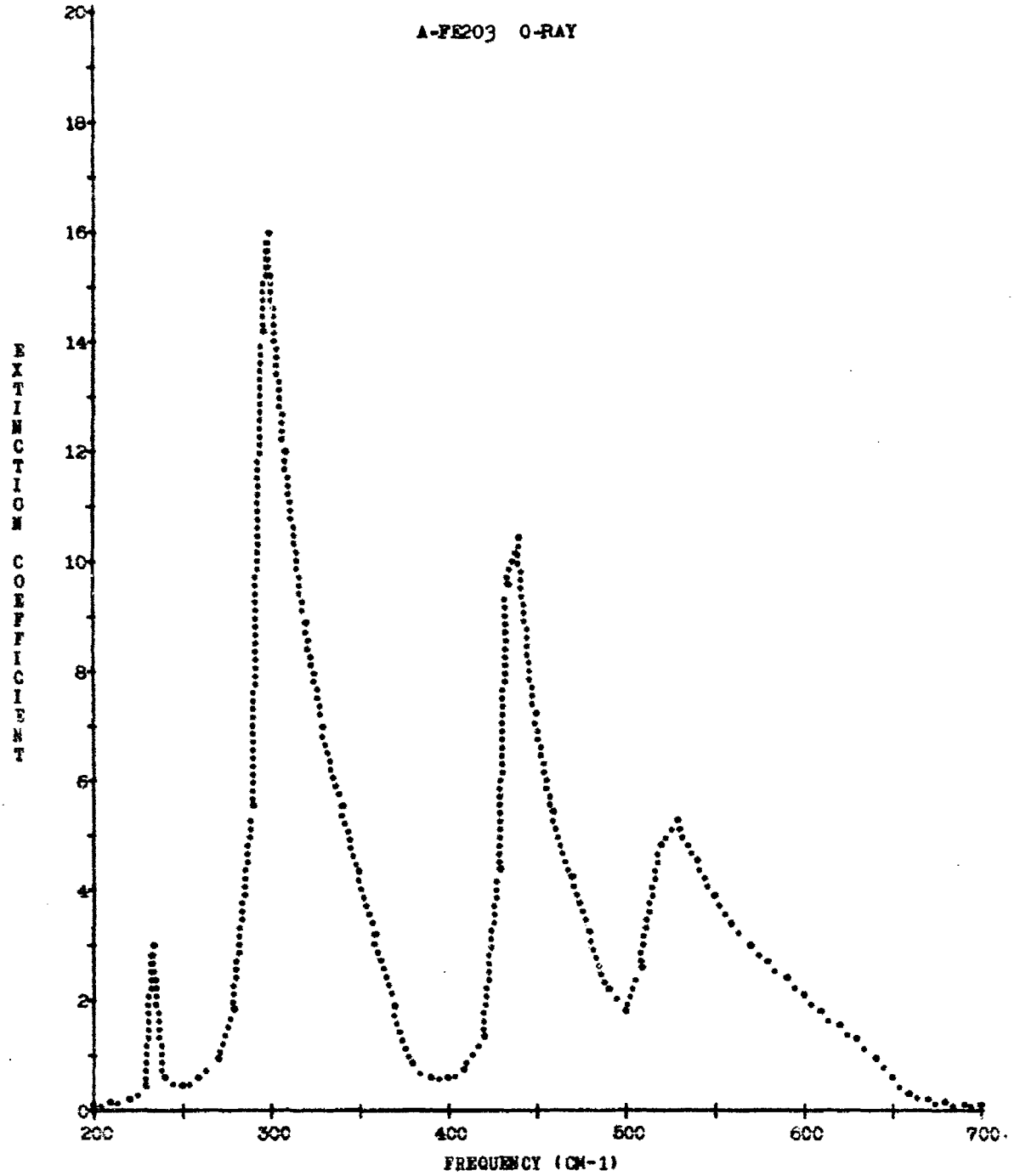

Fig. 8. Extinction Coefficient Spectrum of Ordinary Ray of Hematite

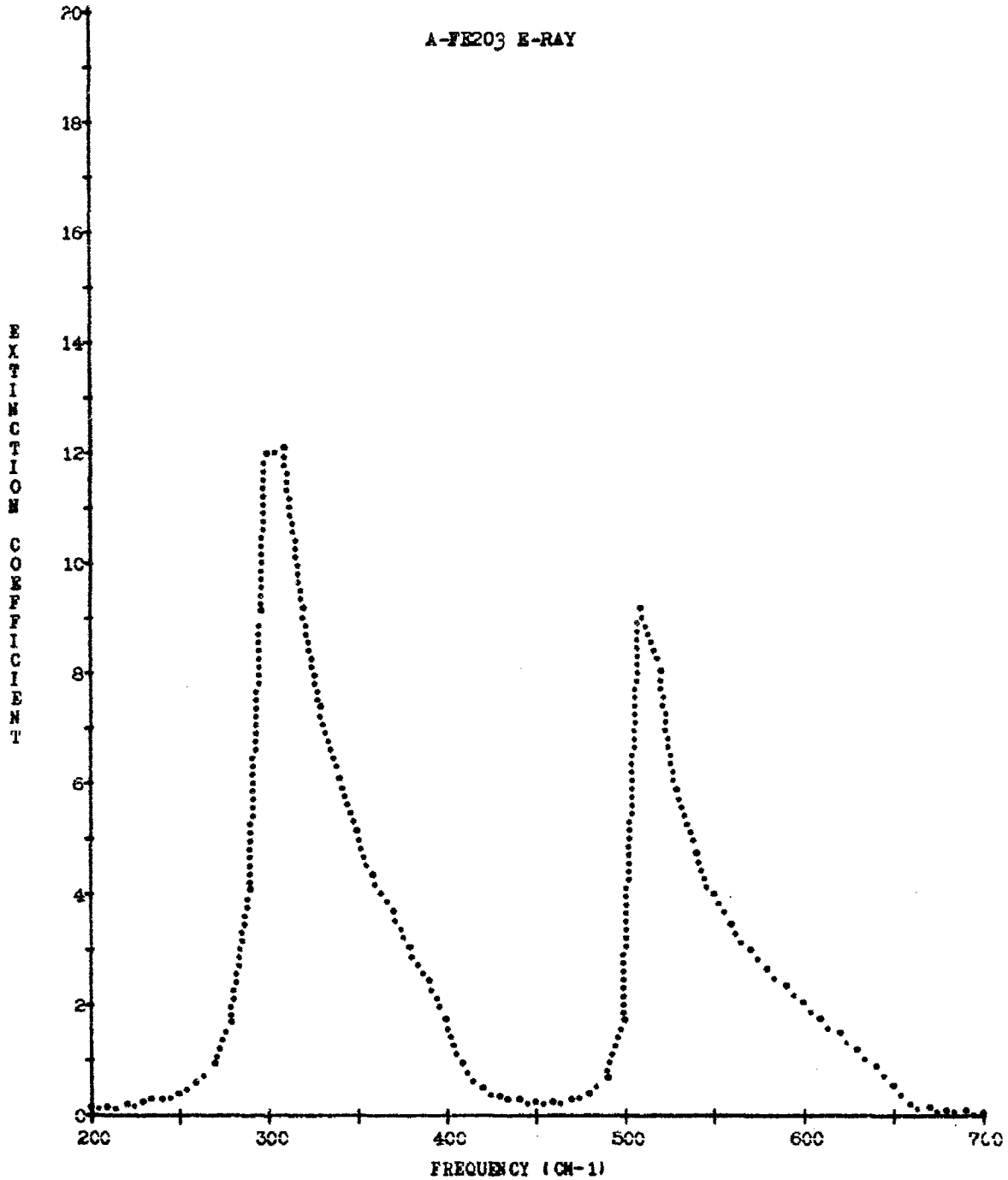

Fig. 9. Extinction Coefficient Spectrum of Extraordinary Ray of Hematite

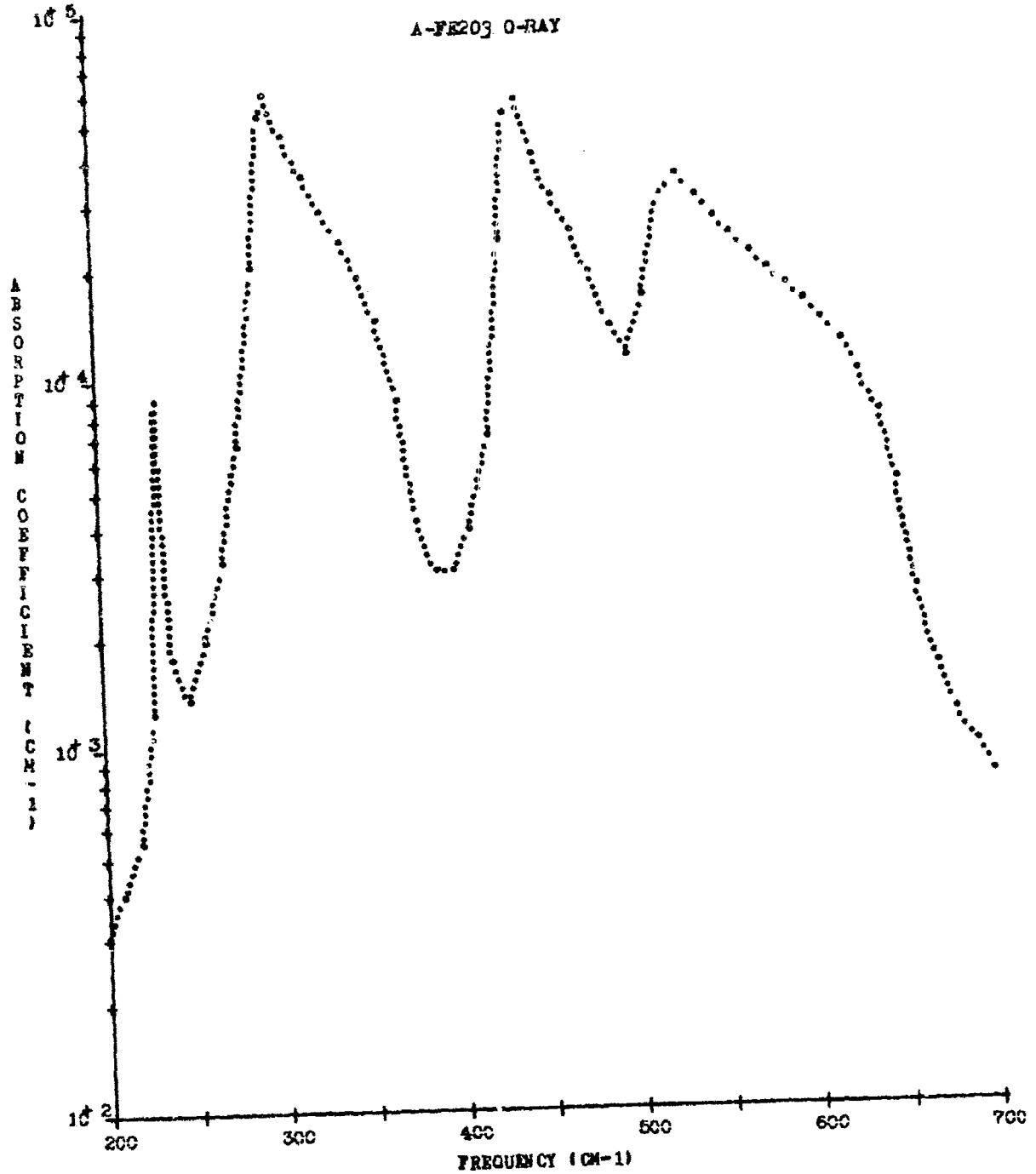

Fig. 10. Absorption Coefficient Spectrum of Ordinary Ray of Hematite

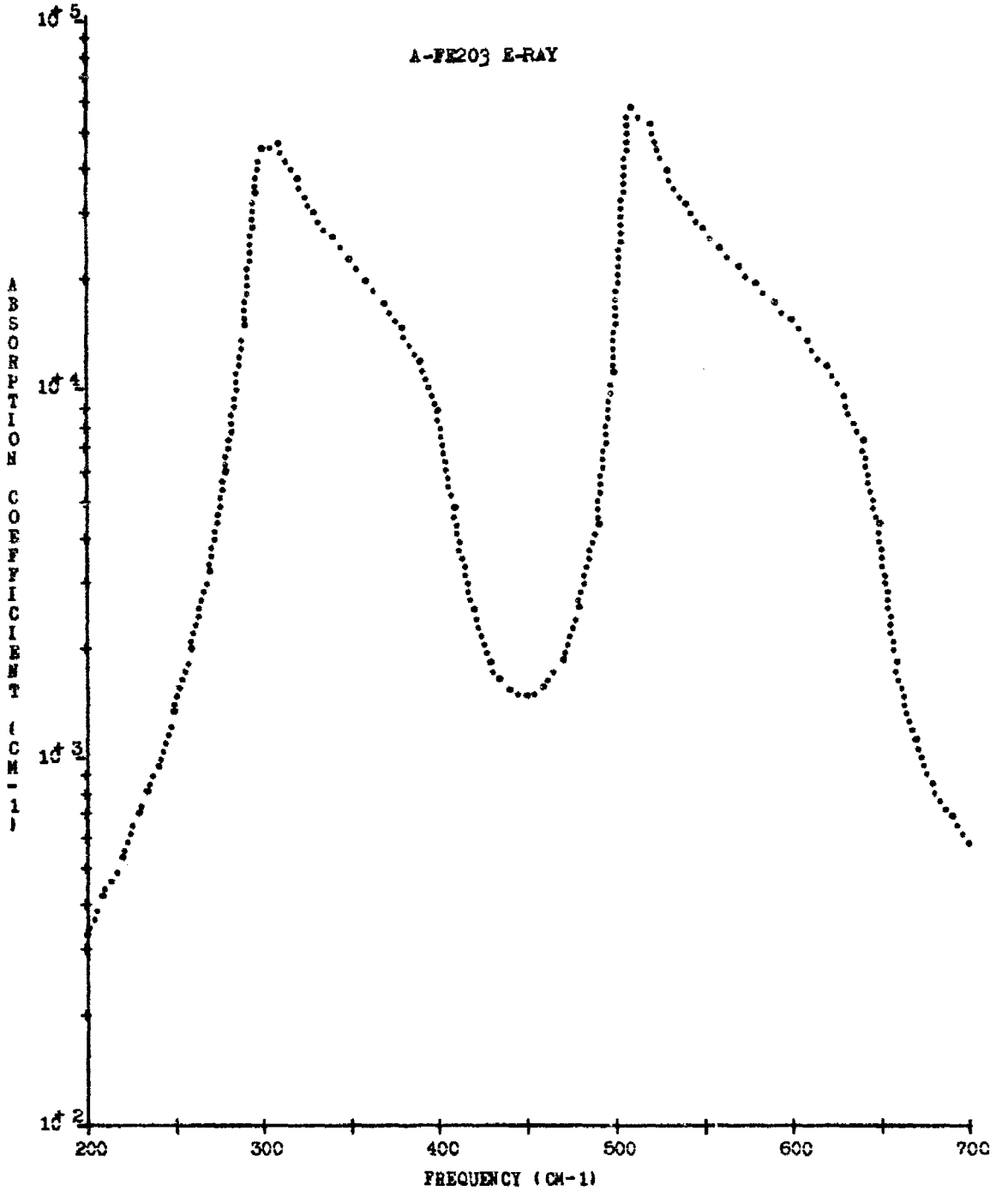

Fig. 11. Absorption Coefficient Spectrum of Extraordinary Ray of Hematite

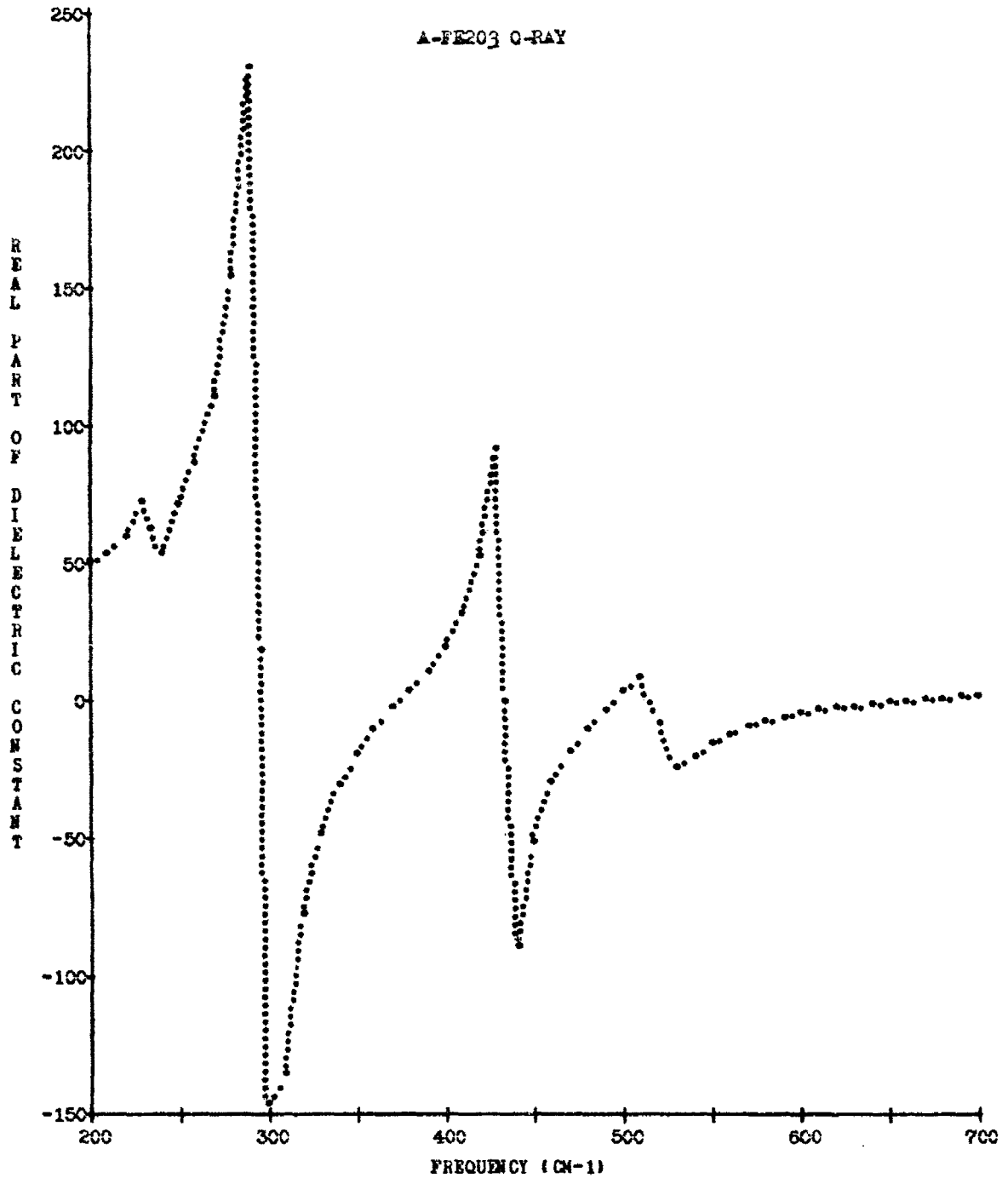

Fig. 12. Spectrum of the Real Part of the Dielectric Constant of Ordinary Ray of Hematite

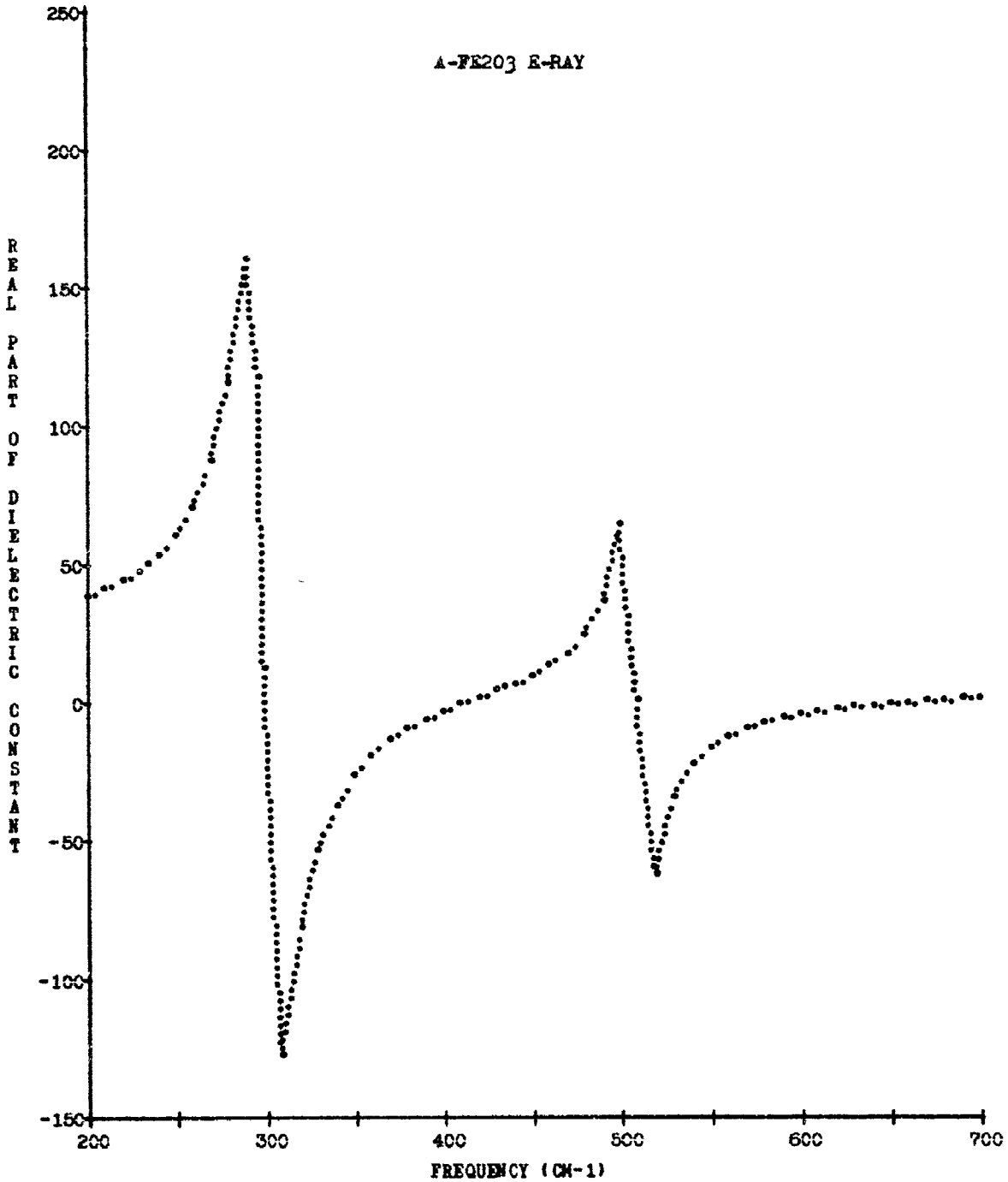

Fig. 13. Spectrum of the Real Part of the Dielectric Constant of Extraordinary Ray of Hematite

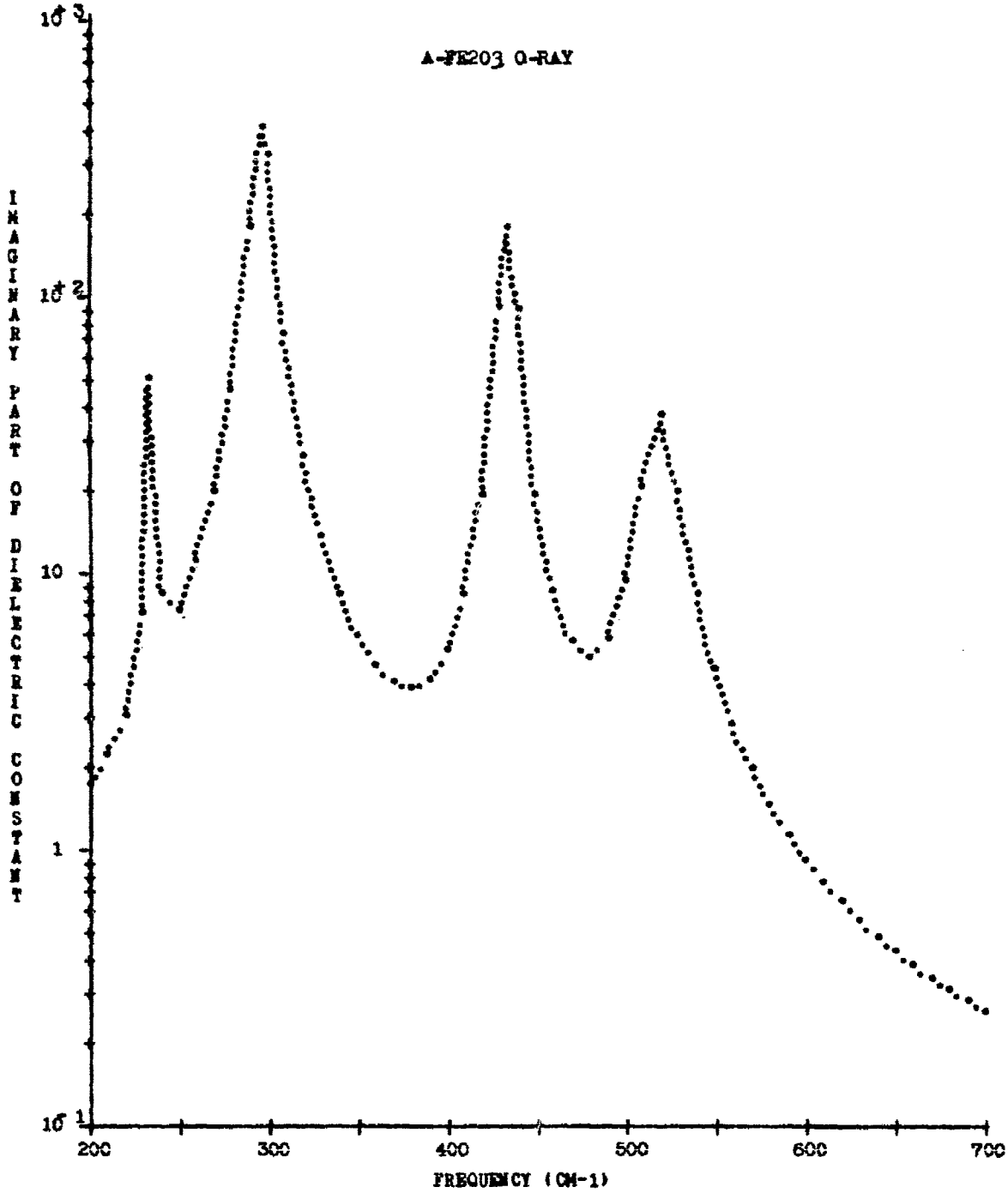

Fig. 14. Spectrum of the Imaginary Part of the Dielectric Constant of Ordinary Ray of Hematite

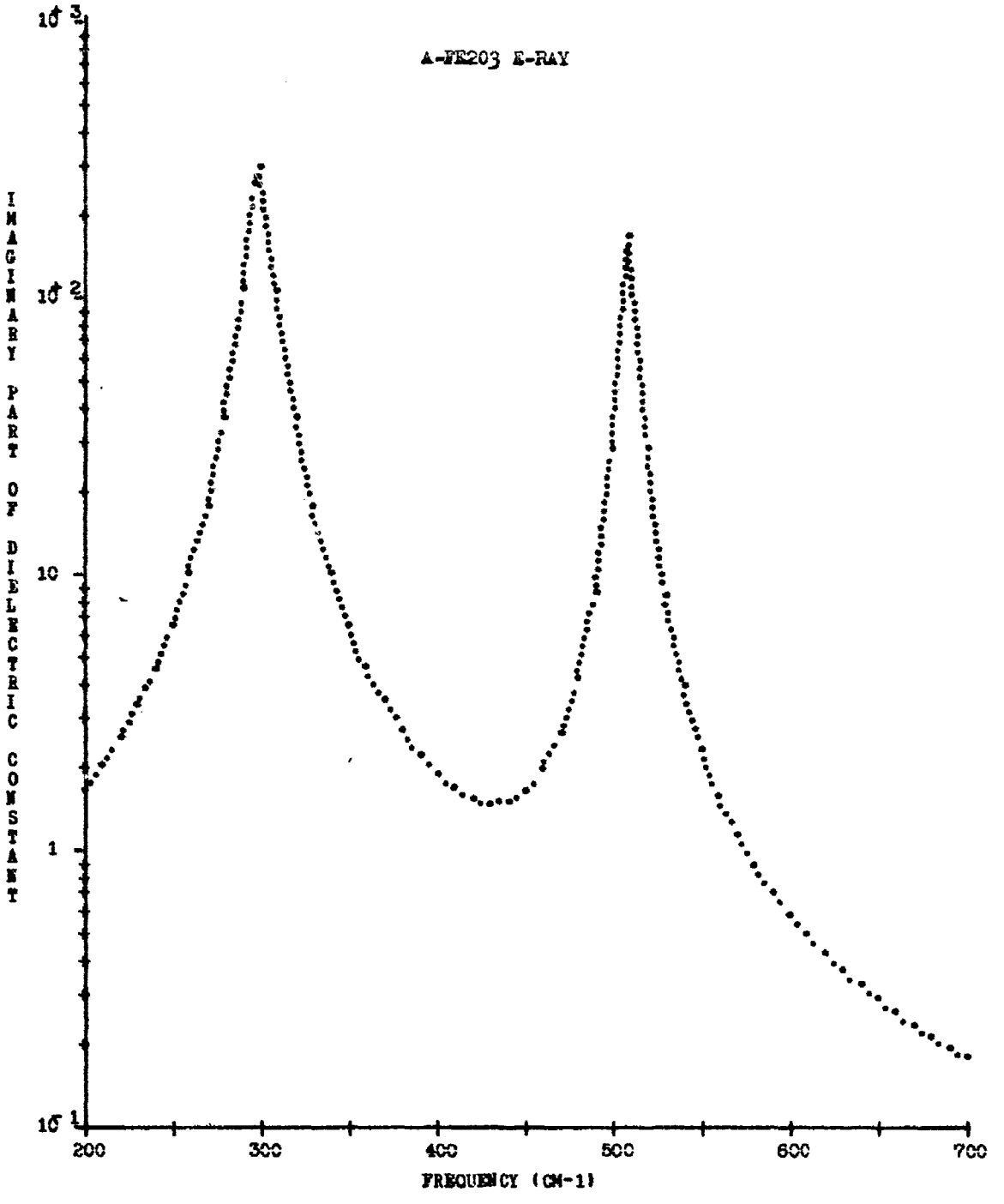

Fig. 15. Spectrum of the Imaginary Part of the Dielectric Constant of Extraordinary Ray of Hematite

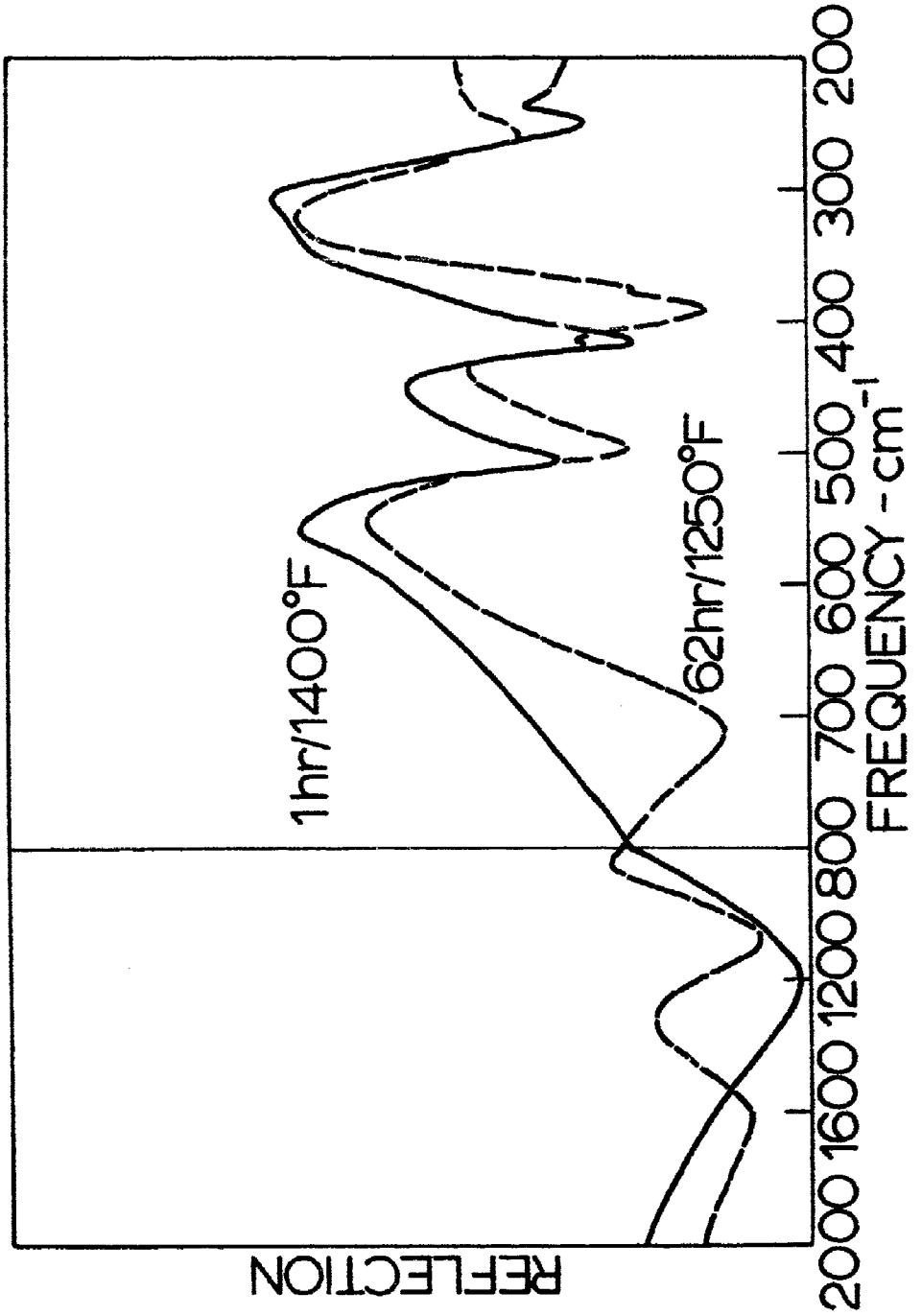

Fig. 16. Reflection Spectra of Oxidation Films on Pure Iron

*U.S.Government Printing Office: 1971 — 759-078/115